DOI:
10.1111/j.1460-9568.2010.07322.x

Document Version
Peer reviewed version

EFFECTS OF URETHANE ANAESTHESIA ON SENSORY PROCESSING IN RAT BARREL CORTEX REVEALED BY COMBINED OPTICAL IMAGING AND ELECTROPHYSIOLOGY

Journal:	*European Journal of Neuroscience*
Manuscript ID:	EJN-2010-03-16720(R)(R).R1
Manuscript Type:	Research Report
Date Submitted by the Author:	26-Apr-2010
Complete List of Authors:	Devonshire, Ian; University of Oxford, Pharmacology Grandy, Thomas; University of Oxford, Pharmacology Dommett, Eleanor; The Open University, Life Sciences; Oxford University, Pharmacology Greenfield, Susan; University of Oxford, Pharmacology
Key Words:	rodent, Voltage-sensitive dye, Somatosensory cortex

Journal Section: Neurosystems
Associate Editor: Laszlo Acsady

EFFECTS OF URETHANE ANAESTHESIA ON SENSORY PROCESSING IN RAT BARREL CORTEX REVEALED BY COMBINED OPTICAL IMAGING AND ELECTROPHYSIOLOGY

Running title: Imaging and electrophysiology of rat barrel cortex

Ian M. Devonshire[a*], Thomas H. Grandy[a], Eleanor. J. Dommett[b], Susan. A. Greenfield[a]

[a]Department of Pharmacology, University of Oxford,
Mansfield Road, Oxford, OX1 3QT.

[b]Department of Life Sciences, The Open University, Walton Hall,
Milton Keynes, MK7 6AA.

Key words: voltage-sensitive dye imaging, somatosensory, rodent

36 pages + 8 figures

Word count: abstract = 165; introduction = 378; materials and methods= 1875; results = 1415; discussion: 2176. Total = 6009.

* Corresponding author.
Telephone: +44 (0) 1865 271624
Fax: +44 (0)1865 271853.
E-mail address: ian.devonshire@pharm.ox.ac.uk (I. M. Devonshire)

Abstract

Spatiotemporal dynamics of neuronal assemblies evoked by sensory stimuli have not yet been fully characterised, especially the extent to which they are modulated by prevailing brain states. In order to examine this issue, we induced different levels of anaesthesia, distinguished by specific electroencephalographic indices, and compared somatosensory-evoked potentials (SEPs) with VSDI responses in rat barrel cortex evoked by whisker deflection. At deeper levels of anaesthesia, all responses were reduced in amplitude but, surprisingly, only VSDI responses exhibited prolonged activation resulting in a delayed return to baseline. Further analysis of the optical signal demonstrated that the reduction in response amplitude was constant across the area of activation, resulting in a global down-scaling of the population response. The manner in which the optical signal relates to the various neuronal generators that produce the SEP signal is also discussed. These data provide information regarding the impact of anaesthetic agents on the brain and show the value of combining spatial analyses from neuroimaging approaches with more traditional electrophysiological techniques.

Introduction

A wide range of brain functions including sensory processing, motor performance, cognition and even sleep are now believed to be dependent on the transient activation of groups of spatially-segregated neurons, 'neuronal assemblies' (Nicolelis *et al.*, 1997; Greenfield, 2000; Harris, 2005; Koch & Greenfield, 2007; Krueger *et al.*, 2008; Shirvalkar, 2009). The concept of neuronal assemblies, first advanced by Donald Hebb (Hebb, 1949), offers a means by which the firing patterns of neurons – or their sub-threshold correlates (Grinvald *et al.*, 2003) – can be correlated with behavioural functions at a population level, thereby extending previous theories of information processing using rate and/or temporal coding patterns (Lin *et al.*, 2006). The advent of imaging techniques such as voltage-sensitive dye imaging (VSDI) (Shoham *et al.*, 1999; Petersen *et al.*, 2003; Grinvald & Hildesheim, 2004; Ferezou *et al.*, 2006; Wu *et al.*, 2008; Chemla & Chavane, in press) has provided experimental evidence to support the above theories and has led to a new appreciation of the importance of spatial parameters of neuronal activity. The subtle yet functionally distinct levels within general anaesthesia could be a valuable tool to investigate assembly function, offering, as it does, a means by which levels of global background activity can be modified to study the relationship between ongoing and sensory-evoked activity. Although reports have suggested that spatiotemporal patterns of neuron firing may underpin the action of general anaesthetics (Cariani, 2000; Greenfield, 2000; Buzsaki & Draguhn, 2004), the influence that different levels of anaesthesia may have on the spatiotemporal dynamics of sensory-evoked activity has yet to be evaluated with VSDI.

The objective of the present study was to characterise state-dependent modulation of sensory responses, produced by changing the level of anaesthesia, using VSDI as a complement to somatosensory-evoked potential (SEP) recordings. Responses were evoked in rat primary somatosensory (barrel) cortex by deflection of a single mystacial whisker on the contralateral snout. The barrel cortex is well-suited to the current study as a relatively circumscribed area of cortex can be stimulated, from which the spread of activity can be clearly visualised and compared between conditions. Individual evoked responses were categorised according to the pre-stimulus cortical state, measured using electroencephalography (EEG), differences in which were produced by administering supplemental doses of anaesthetic to produce discrete and clearly identifiable levels of anaesthesia.

Materials and methods

Animals and Surgical procedures

Female Wistar-Han rats (HsdHan:WIST; n = 7) weighing between 210-260 g were used (Harlan, Bicester, UK) and kept on a 12-hr dark/artificial-light cycle in an open-system holding room at a temperature of 22°C, humidity 55%; food (RM3p, Special Diets Services Ltd.; Witham, UK) and water were available *ad libitum*. The experiments described were approved by the local University ethical committee and all procedures were performed with Home Office approval under the Animals (Scientific Procedures) Act 1986.

Rats were anaesthetised with urethane (1.15 g/kg) and chloral hydrate (0.16 g/kg) and transferred to a stereotaxic frame (David Kopf Instruments, Tujunga, CA, USA). In order to modulate the depth of anaesthesia during the data acquisition phase, supplementary doses of urethane were injected (20% of original dose each time) until the required level was achieved. Respiratory and cardiovascular parameters were recorded throughout surgical and experimental procedures. Rate and depth of respiration were recorded using a custom-built monitor based around an accelerometer integrated circuit (Devonshire *et al.*, 2009). Heart rate was recorded via single-strand copper electrocardiogram (ECG) recording leads inserted subcutaneously behind each forelimb and connected to a custom-built ECG-processing unit. A craniotomy was performed over the primary somatosensory cortex at the following approximate stereotaxic co-ordinates: anterior-posterior = 1-5 mm, medial-lateral = 4-8 mm. A single trepanne hole (~1 mm Ø) was drilled in the left frontal bone into which a short loop-tipped silver wire electrode (0.2 mm Ø; Intracel,

Royston, UK) was inserted to act as a reference electrode. An imaging chamber comprising a 3 mm section of a disposable 5 ml syringe (Becton-Dickinson; Oxford, UK) was cemented in place around the craniotomy using dental cement (Duralay, Reliance Dental; Worth, IL, USA).

Sensory stimulation

All whiskers on the left-hand side of the snout were trimmed apart from whisker C2. The remaining whisker was stimulated 3 mm from its base by a 26G hypodermic needle attached to a piezoelectric wafer (PL122.11, Physik Instrumente; Harpenden, UK). Displacement of the wafer was produced by applying an electrical potential across it (10v for 20ms) to give approximately 2 mm of movement in a caudal direction. Whiskers were deflected for 1 s at 2 Hz and 10 Hz in a randomly interleaved pattern; trials were separated by 60 s and a total of 144 trials were presented to each animal over a period of 4 hours.

Optical Imaging

The barrel cortex was stained with a styryl dye (Di-4-ANEPPS, Invitrogen; Paisley, UK) at a concentration of 0.2mM through an intact dura. To the best of our knowledge, there have been no reports of Di-4-ANEPPS staining having produced adverse effects (i.e. pharmacological side effects or photodynamic damage) in neural tissue used for VSDI studies. Nevertheless, we explored this possibility in our own preliminary investigations: when compared to pre-staining baseline recordings, Di-4-ANEPPS at a concentration of 0.2 mM was found to produce no changes in either the amplitude or profile of SEPs after an application time of 60 min. Furthermore, response profiles remained stable for over 4

hours after staining and no parameters fluctuated significantly over the course of imaging; data at start and end of imaging: SEP response amplitude = -5.38 mV versus -4.71 mV; VSDI response amplitude = 0.184% versus 0.202% (paired ttest, p = 0.38); number of pixels activated above threshold = 4355 versus 5243 (paired ttest, p = 0.43); heart rate = 485 versus 488 BPM (paired ttest, p = 0.76). These data also confirm the physiological stability of the preparation used and the validity in using increasing depths of anaesthesia rather than either randomly interleaved (which would be impossible with the chosen anaesthetic due to its long duration of action) or one depth of anaesthesia per animal (which would use an unnecessary number of animals and not be in accordance with national guidelines to reduce animal usage (UK Home Office; Research and Testing Using Animals; www.homeoffice.gov.uk/science-research/animal-testing; accessed 10th January 2010. National Centre for the Replacement, Refinement and Reduction of Animals in Research; www.nc3rs.org.uk; accessed 10th January 2010). During acquisition, the cortex was illuminated with 530 ± 10 nm light and passed through a > 590 nm high-pass filter. A complementary metal oxide semiconductor imaging system (BrainVision Ultima; Tokyo, Japan) with an array of 100x100 was used to detect emitted light. In each stimulation trial, frames were recorded at 500 Hz for 2.3 s with a pre-stimulus period of 0.5 s. A brief initial imaging session (consisting of 5 stimulation trials) was performed in order to locate the maximal site of activation, position the imaging camera appropriately and aid in the positioning of the SEP recording electrode.

Electrophysiology

Electrophysiological recordings and optical imaging were performed concurrently. SEP (and EEG) recordings were made with a single platinum-iridium electrode (25µm

diameter; FHC; Bowdoin, ME, USA). The electrode was placed on the surface of the dura at the centre of the evoked optical activity, following an initial imaging session. The EEG/SEP signal was processed via a NeuroLog head-stage, pre-amplifier and filter module (NL100AK, NL104A, NL125; Digitimer; Welwyn Garden City, UK), high-pass filtered above 0.5 Hz and displayed in Spike2 software via a microCED1401 data acquisition unit (Cambridge Electronic Design; Cambridge, UK).

Assessment and modulation of anaesthetic depth

Discrete levels of anaesthesia in rodents anaesthetised with urethane or halothane have already been categorised by Friedberg and colleagues on the basis of EEG spectral components (Friedberg *et al.*, 1999). These levels were designated I – IV after the original work of Guedel (Guedel, 1920), with level I representing the awake state and level IV anaesthesia marked by an isoelectric EEG. Level III is deemed appropriate for surgery and is divided into 4 further sub-levels, each of which are identifiable by eye and by assessing dominant spectral components; levels that were identified in the present study were III-2, III-3 and III-4 (III-4 being the deepest level). Urethane anaesthesia typically consists of episodes of different levels (Angel *et al.*, 1976; Friedberg *et al.*, 1999), with one level able to give way to another without any intervention. As such, each individual stimulation trial was categorised according to the spectral components of its pre-stimulus EEG (a period of 5 s in duration). A fast Fourier transform was calculated and the mean power frequency obtained. Mean power frequencies above 2.5 Hz were reliably identified as level III-2 anaesthesia, referred to as ‘light’; frequencies below 1 Hz were reliably level III-4, referred to as ‘deep’, and all other frequencies categorised as III-3, referred to as ‘moderate’.

Data analysis

Noise in the imaging data produced by cardiovascular pulsations was not removed by triggering data acquisition from ECG waveforms and subtracting images obtained from null stimulus trials, as is customary in many VSDI analyses (Petersen *et al.*, 2003), but by using an algorithm based on that previously reported by Jian-Young Wu and colleagues (Lippert *et al.*, 2007). Briefly, the ECG was recorded simultaneously with each imaging acquisition and an "average pulsation artefact" generated on a pixel-by-pixel basis centred on the ECG 'R' wave. Pulsation noise was then removed from the imaging signal by subtracting the artefact template; there was no deterioration in the imaging signal as demonstrated by spectral analyses which showed only the heart-rate frequency was affected (Ma *et al.*, 2004; Lippert *et al.*, 2007). The advantage of removing cardiovascular noise in this manner is a reduction in light exposure due to a 50% reduction in the number of trials which are necessary to obtain response data for a given stimulus presentations. This reduces the overall risk of photodynamic damage and bleaching.

Both SEP and imaging trials were separated on the basis of network state, based on the mean power frequency of the pre-stimulus EEG (described above). SEP data was then band-pass filtered between 1-250 Hz; imaging data was high-pass filtered above 1 Hz and a Gaussian spatial filter applied to the imaging data (15x15; sigma = 2). Temporal information was extracted from the imaging data by using a circular region-of-interest (ROI) centred on the pixel with maximum activation. This ROI was entirely contained within the C2 barrel (shown by post-mortem histological analysis). Temporal data

segments from both SEP and VSDI were averaged into three individual response types: a *stand-alone* response, obtained from the first response to the 2 Hz stimulus; a *low-frequency* response, obtained from the second response to the 2 Hz stimulus; and a *high-frequency* response, obtained from averaging the final six responses to the 10 Hz stimulus.

It was anticipated from previously published results that multiple response components would be observable in both SEP and imaging data sets: four components in SEP data (composed of two positive and two negative waveforms; (Di & Barth, 1991)) and two components in imaging data (one positive and one negative; (Derdikman *et al.*, 2003)). For each component in both data sets, the maximum amplitude and latency-to-peak were obtained. SEP response components alternate between positive and negative; hence, for all but the first component, response amplitudes were calculated from the amplitude of the previous waveform, i.e. amplitude represents the vertical distance between adjacent components. Maximum amplitudes in the SEP data were obtained within the following time windows: 0-20 ms, 10-25 ms, 20-50 ms, 40-100 ms. VSDI response components were all calculated from zero. Maximum VSDI amplitudes were obtained within 0-40 ms (positive) and 50-300 ms (negative; 50-100 ms for the negative response evoked at high-frequency due to the interval between successive 10 Hz stimuli).

An overall measure of the 'size' of the spatial response was obtained by calculating the number of pixels activated above a pre-defined threshold (20% of the maximum response that was elicited in that animal across all three levels of anaesthesia) while the three-

dimensional 'shape' of the response was obtained by locating the pixel with maximum activation in each animal, bisecting the image in two dimensions (vertical and horizontal) centred on this pixel and averaging the resultant vectors. One-way analyses of variance were performed and followed by least significant difference post-hoc tests where appropriate.

Histology

One animal from the study was used to compare spatial responses with the underlying cortical anatomy, i.e. layer IV barrels. After the experiment, animals were sacrificed by an overdose of Pentobarbitone (Pentoject, Animalcare Ltd.; York, UK) and perfused transcardially with saline. The brain was removed and immersed in 4% paraformaldehyde for three days at which time the right barrel cortex was dissected from underlying structures. The cortex was then lightly pressed for 24 hours before 100 μm thick tangential slices were removed using a vibratome (VT1000S, Leica Microsystems; Milton Keynes, UK). To visualise the relative distribution of cytochrome oxidase activity and reveal the layer IV barrels (Land & Simons, 1985), the slices were incubated for ~8 hours at 37ºC in 0.1M sodium phosphate buffer solution containing 0.2 mg/ml cytochrome C, 0.67 mg/ml diaminobenzidine and 27 μg/ml sucrose. Slices were then mounted onto gelatin-coated slides, dehydrated and cover-slips attached using Entellan. Unless otherwise stated, all chemicals were obtained from Sigma-Aldrich (Poole, UK). A warping algorithm originally devised by John Mayhew and colleagues (Zheng *et al.*, 2001) was used to match histology and VSDI images together. Using corresponding points within each image, normally the penetration marks of large blood vessels that are

traceable in histological sections as well as VSDI images, functional maps could be placed on to histological sections; for methodological details see (Zheng *et al.*, 2001).

Results

Three levels of anaesthesia could be consistently obtained from the animals under urethane anaesthesia in the present study and are illustrated in figure 1A-C. It is important to note that all anaesthetic levels belong to the category of 'surgical anaesthesia', i.e. characterised by a level of sedation and analgesia suitable for the performance of invasive surgical procedures (Guedel, 1920; Friedberg *et al.*, 1999). Supplementary injections of urethane were administered throughout the day in order to produce the range of levels shown (figure 1A-C). Typically, 20% of the original dose produced shifts from light to moderate anaesthesia or from moderate to deep anaesthesia. Urethane anaesthesia is known to occasionally drift between individual levels, therefore the particular level in which each stimulus was presented was characterised off-line following the experiment, using the pre-stimulus EEG. All three levels were obtained from all animals used in the study and, within each animal, an equal number of trials was averaged and analysed from each level (between 8-12). The average fast Fourier transforms from all trials in each anaesthetic level are shown in figure 1D. The categorisation of different anaesthetic levels according to mean power frequency of the EEG reliably enabled fast and efficient sorting of trials. This was confirmed visually by the presence of burst-suppression of trials during deep anaesthesia (figure 1C), and a large reduction in EEG waveform amplitudes of trials during light anaesthesia (figure 1A).

Electrophysiology versus optical imaging: temporal parameters

Average SEP and VSDI responses elicited from a single animal in response to whisker deflection are shown in figure 2. The upper panel (A-C) shows the cortex illuminated by

530nm light together with a snapshot of the activation elicited by the stimulus (and the region-of-interest from which time course data was obtained) and the pixels that are supra-threshold at this same time point. The inset of figure 2B displays the shape of the response, obtained by locating the pixel with maximum activation, bisecting the image horizontally and vertically across this pixel and averaging the resultant vectors (used later to characterise the shape of the evoked activity at different anaesthetic levels). The lower panel (D-F), in turn, provides time courses of the SEP, VSDI and spatial activation. Figure 2D also show the four components of the SEP response (P1, N1, P2, N2) while figure 2E shows the two components of the VSDI response (positive and negative); both illustrating how the latencies and amplitudes were calculated for each response component. To facilitate analysis, data were divided into three different response *types*: responses to stand-alone, low-frequency and high-frequency stimulation. The origin of these response types are illustrated in figure 3 in which whole time courses of average responses to stimuli presented at 2 Hz and 10 Hz from all animals during light anaesthesia are shown.

Time courses of average SEP and VSDI responses during all levels of anaesthesia are shown in figure 4, from which amplitude data have been extracted and are shown in figure 5. In order to compare between SEP and VSDI data, and between different response components and stimulation frequencies, data in figure 5 are shown in relation to the response evoked during light anaesthesia. The most noticeable effect of anaesthesia is a dose-dependent reduction in amplitude of all SEP and VSDI response components which was most marked in response to high-frequency stimulation (e.g. figure 5C versus

5A). Compared to light anaesthesia, the average amplitudes of all SEP response components to high-frequency stimulation (figure 4C & 5C) was reduced by 45 (± 12) % and 78 (± 6) % in moderate and deep levels, whereas the SEP responses to stand-alone (figures 4A & 5A) and low-frequency stimulation (figure 4B & 5B), were only reduced by 28 (± 11) % and 27 (± 12) % in moderate anaesthesia and 49 (± 10) % and 52 (± 11) % in deep anaesthesia. F and p values for SEP stand-alone response components N1 and P2: 8.519, $p < 0.01$; 9.124 $p < 0.01$; for low-frequency response components N1, P2 and N2: 8.252, $p < 0.01$; 7.673, $p < 0.01$; 11.673, $p < 0.01$; for all high-frequency response components: 7.651, $p < 0.01$; 5.446, $p < 0.05$; 6.537, $p < 0.01$; 10.439, $p < 0.01$. Overall, VSDI responses did not exhibit as great a reduction in amplitude as the SEP responses. Nevertheless, responses to high-frequency stimulation (figure 4F & 5F) again showed the greatest reductions in response amplitudes: both positive and negative response components were reduced, on average, by 32 (± 9) % and 41 (± 9) % in moderate and deep anaesthesia compared to the response in light anaesthesia. Response amplitudes to stand-alone (figure 4D & 5D) and low-frequency stimulation (figure 4E & 5E) showed similar reductions: the stand-alone and low-frequency VSDI responses were reduced, on average, by 12 (± 10) % and 19 (± 7) % in moderate anaesthesia and by 29 (± 10) % and 34 (± 11) % in deep anaesthesia. F and p values for VSDI stand-alone negative response: 3.797, $p < 0.05$; for low-frequency negative response: 8.299, $p < 0.01$; for high-frequency positive response: 3.850, $p < 0.05$.

As anaesthetic level became deeper, changes in SEP and VSDI response latencies (for any response component) were not as widespread as was observed for changes in

amplitude, and no significant changes were observed among anaesthetic levels. However, the time taken to return to baseline was noticeably longer for the positive VSDI response: the duration before the response crossed the baseline in light, moderate and deep anaesthesia in the stand alone stimulus was 38.3 (± 3.7), 47.7 (± 5.7) and 68.0 (± 8.7) ms (results of one-way ANOVA: $F=5.644$, $p < 0.05$; least significant difference post-hoc test found statistical difference between light and deep anaesthesia, $p < 0.05$).

Spatial parameters of the optical response

The maximum area of cortical activation, calculated as the number of pixels above a pre-determined threshold, was reached ~2-4 ms after the time at which the optical signal reached its peak at the centre of the stimulated barrel. Figure 6A displays snapshots of the spatial extent of activation at discrete time frames in response to stand-alone stimulation during light anaesthesia, averaged across all animals by centralising to the maximally-activated pixel; figure 6B displays the same data during deep anaesthesia. Data were also normalised to the maximally activated pixel. During light anaesthesia, an initially localised area of activity gives way to more widespread activity that fills the whole image region within a relatively short period of time (~12ms). This is followed by an extensive hyperpolarisation that occurs later in the activated barrel then elsewhere (see activity at 60ms) and, in some regions, lasts up to 200ms after stimulation onset. Spatial activity in deep anaesthesia follows the same overall pattern of focal depolarisation, propagation over the entire region and subsequent hyperpolarisation, but differs in several ways to the response under light anaesthesia: firstly, the initial depolarisation is of a smaller amplitude (as noted during examination of the VSDI time course data from a ROI within the activated barrel; figure 4D-F & 5D-F), and does not extend as widely; the subsequent

hyperpolarisation is also of a smaller amplitude and lasts for a shorter duration. The same pattern of activity was observed in response to low- and high-frequency stimulation apart from the effect on duration at high-frequencies which, due to the short interval between subsequent stimuli (100ms) the large and extensive hyperpolarisation did not develop strongly.

The above spatial observations in response to stand-alone stimulation were confirmed quantitatively by obtaining pixel activation counts, calculated using a specific threshold (figure 7). Anaesthesia had a dose-dependent suppressive effect on the spread of both depolarising and hyperpolarising waves in response to stand-alone (figure 7) as well as low-frequency sensory stimulation. It was previously observed in the time course of the VSDI signal obtained from a ROI centred over the activated barrel (figure 3C & D, 4D-F, 5D-F) that the initial depolarisation was of a much greater magnitude, although a shorter duration, than the later hyperpolarisation. Nevertheless, examination of the spatial spread of the optical signal indicates that, although of a small magnitude, the hyperpolarisation is almost as extensive in space throughout its long duration as the initial depolarisation phase (figure 7A). There were no observed differences in the number of pixels undergoing depolarisation or hyperpolarisation in response to high-frequency stimulation during the different levels of anaesthesia. This was due to the weakness in the evoked signal at this stimulation frequency that resulted in a poor signal-to-noise ratio across the captured image.

The above analysis does not address whether the internal dynamics of the assembly, the net size or response shape, has changed. To resolve this question, the pixel with maximal activation within the first 12 ms of the stand-alone response was located in each animal, bisected in vertical and horizontal dimensions and averaged (figure 8C). This provided an outline of the shape of the assembly (from centre to periphery) obtained during each level of anaesthesia. Figure 8C illustrates the differences between the activity in light, moderate and deep anaesthesia; there were no differences found between the shape of the evoked response in the different levels of anaesthesia during this depolarisation phase of the response (that is, there was no difference between the curves when amplitude was taken into account). We were unable to assess the shape of the activation during the hyperpolarisation phase as it was largely abolished by deep anaesthesia (see figures 4D and 6). Figure 8A illustrates the localisation of the initial response in relation to the underlying cortical anatomy (layer IV barrels; figure 8B) to demonstrate concordance between the imaging signal and the activated barrel.

Discussion

The most striking and consistent change observed in the cortical responses evoked by multi-frequency sensory stimulation in the current study was a anaesthetic dose-dependent reduction in response amplitude. This was recorded at all stimulation frequencies, observed in all response components, and was greatest when responses were evoked by high-frequency sensory stimulation. Response latencies were also most influenced by anaesthetic depth during high-frequency stimulation but did not exhibit as robust or uniform changes as did changes in amplitude. Anaesthesia also prolonged early components of evoked responses and decreased the overall area of cortex that was activated. Despite the above changes, the shape of the VSD response (i.e. the three-dimensional VSDI signal) remained constant at different levels of anaesthesia.

What do VSDI and SEP signals measure?

VSDI is now a well-established technique for investigating neuronal function *in vitro* as well as *in vivo* and, in support of this, the resultant optical signals having been repeatedly demonstrated to be highly correlated with local-field and intra-cellular potentials (Contreras & Llinas, 2001; Petersen *et al.*, 2003; Grinvald & Hildesheim, 2004). However, the fidelity between an *in vivo* optical signal and a multi-component SEP cortical response (emanating from multiple neuronal generators) as it travels between different cortical layers (Di & Barth, 1991), such as that used in the current study, has not previously been examined, and therefore warrants a thorough comparison and discussion. The whisker-evoked SEP response is comprised of four individual peak responses, alternating between positive and negative - P1, N1, P2 and N2 - and are typical

waveforms that can be recorded from sensory cortex in a range of species (Goff *et al.*, 1978; Coenen, 1995). However, over the same time-scale, the VSD response is comprised of just two components: a positive (or depolarisation) phase and a negative (or hyperpolarisation) phase, which is in agreement with previously published imaging studies of the barrel cortex (Takashima *et al.*, 2001; Derdikman *et al.*, 2003). The observed difference between electrophysiology and VSDI is not unexpected when one compares the complex origins of evoked potential recordings, which are dictated by cytoarchitecture and properties of extracellular conductance (Nicholson & Freeman, 1975; Mitzdorf, 1985), and the spatial origins of optical imaging signals, which are largely limited to supragranular layers due to dye penetration (Kleinfeld & Delaney, 1996; Petersen *et al.*, 2003; Ferezou *et al.*, 2006) and light scattering in tissue (Mayhew *et al.*, 2000; Grinvald & Hildesheim, 2004). Due to their latency and laminar depth profiles, as previously assessed by current-source density analysis, both P1 and N1 SEP responses are likely to represent monosynaptic and di-synaptic depolarisations of supragranular cells (Devonshire *et al.*, 2007). The P1 response corresponds to the initial thalamocortical input directly onto apical dendrites of supragranular pyramidal cells, and possibly indirectly via layer IV stellate cells, that results in a surface positivity (Mitzdorf, 1985; Di *et al.*, 1990; Sukov & Barth, 1998; Jellema *et al.*, 2004). Stellate cells have a closed-field geometry and, therefore, do not contribute to the surface potential themselves (Di *et al.*, 1990). The N1 component represents further input to the supragranular layers from layer IV (as well as depolarisation of distal apical dendrites of infragranular cells; (Jones, 1984; Mitzdorf, 1985; Sukov & Barth, 1998). In accordance with the supragranular origin of the optical signal and heavy supragranular component of P1 and N1 SEP responses, after

initially reaching its peak at approximately the same time as the P1 response, the depolarisation phase of the evoked VSD signal exhibits a slow decay time that also encapsulates the N1 waveform (see inset of figure 4D).

The P2 and N2 SEP responses are more variable in amplitude (and latency) and have a wider spatial distribution than earlier components (Di & Barth, 1991; Barth *et al.*, 1993). Absence of concurrent multi-unit activity (Kulics, 1982; Kulics & Cauller, 1986) makes the role of these late components ambiguous and they may derive from a combination of $GABA_A$-mediated inhibitory postsynaptic potentials in the supragranular layers and repolarisation mechanisms (Steriade, 1984; Carvell & Simons, 1988; Takashima *et al.*, 2001). This theory is supported by the current findings as the VSD enters the hyperpolarisation phase as the P2 peak is reached and is maintained throughout the N2 response (e.g. figure 4A&D; also see inset of D). The cortical region undergoing hyperpolarisation is also quite extensive (e.g. figure 6A), despite exhibiting a smaller amplitude than that observed in the depolarisation phase (e.g. figure 4D; as also found in (Takashima *et al.*, 2001)).

Optical imaging techniques extend electrophysiological recording approaches by providing spatial information that traditional single electrodes cannot, i.e. data from wider cortical regions that are able to give a more faithful read-out of the collective activity that constitutes a neuronal assembly. Our data demonstrate that the evoked optical response was initially restricted to a single barrel (figures 6 & 7) and then spread to encompass the entire barrel field, before the cortex underwent an extensive and

prolonged hyperpolarisation. The initial spread of activity is likely to be a result of long-range axonal collaterals from supragranular pyramidal cells as well as projections from infragranular layers (Bernardo *et al.*, 1990a; Bernardo *et al.*, 1990b; Egger *et al.*, 1999; Reyes & Sakmann, 1999) which, in the single animal examined and displayed in figure 8, extended more along the whisker row than the arc, in line with previously published findings (Petersen *et al.*, 2003). The subsequent cortical hyperpolarisation, that is thought to be brought about by supragranular $GABA_A$-mediated inhibition (Carvell & Simons, 1988), was observed to encircle the stimulated barrel, similar to that shown previously (Derdikman *et al.*, 2003), and confirms the utility in applying VSDI to examine mechanisms that generate surround inhibition.

Response amplitude and activation area are decreased in deeper levels of anaesthesia

The anaesthetic dose-dependent reduction in response amplitude is consistent with previous electrophysiological findings (Angel & Gratton, 1982; Armstrong-James & George, 1988; Koyanagi & Tator, 1996; Erchova *et al.*, 2002; Antunes *et al.*, 2003) and adds to the growing body of literature that show state-dependent changes in the temporal profile of evoked responses (Sachdev *et al.*, 2004; Haider *et al.*, 2007; Hasenstaub *et al.*, 2007; Kuhn *et al.*, 2008). A reduction in overall activity in the cortex (i.e. anaesthesia-induced reduction in response magnitudes, figure 4, with putative thalamocortical response components such as P1 exhibiting no greater or lesser response than intracortical responses such as N1; figure 5A-C) is likely to be due to an inhibition of the initial inputs from cells in the ventro-posterior medial nucleus (VPM) of the thalamus (known to occur during deep anaesthesia; (Aguilar & Castro-Alamancos, 2005)), which have been hyperpolarised due to direct anaesthetic action on $GABA_A$ or activation of K+

channels (Franks, 2008) or by a reduced cholinergic input to the thalamus from the basal forebrain (Castro-Alamancos, 2004). Reduced acetylcholine may also simultaneously work directly in the cortex to decrease response amplitude (Oldford & Castro-Alamancos, 2003). In any event, reduced sensory responsiveness is so widely observed during anaesthesia that it has served as a feedback signal in automated anaesthetic-delivery systems (Angel *et al.*, 2000).

Responses evoked by high-frequency stimulation underwent proportionally greater reductions in amplitude than stand-alone or those evoked by low-frequency stimulation (figure 5A-C). As stimulus frequency is increased, average response amplitudes decrease (Ngai *et al.*, 1999; Castro-Alamancos, 2004) as a result of a combination of recurrent inhibition from the reticular nucleus to thalamic projection cells, inhibition of post-synaptic Ca^{2+} channels through activation of metabotropic glutamate receptors, depletion of neurotransmitter and desensitisation of post-synaptic receptors (Lee *et al.*, 1994; Castro-Alamancos, 2004). This has the added effect of making the generation of action potentials less likely, by reducing the magnitude of excitatory post-synaptic potentials to a point close, or below, a cell's firing threshold, and may explain the greater reduction in response amplitude at high-frequency stimulation.

There is no clear consensus for the impact of anaesthesia on response latency with positive (Kisley & Gerstein, 1999; Schmidt *et al.*, 2007) and negative results being reported (Goss-Sampson & Kriss, 1991; Freye *et al.*, 2004) in the literature; our results also indicate no clear effect. Late SEP components of the response to high-frequency

stimulation decreased in latency, but this is likely due to the small amplitude of these responses resulting in shorter overall response durations.

Another observation from the data in this study was that, despite a reduction in the amplitude of sensory-evoked responses at deeper levels of anaesthesia, the overall duration of the response, i.e. the time taken for activity to cross baseline, was prolonged (figure 4D&E). Such sustained activity has also been recorded during the 'silent' periods of level III-3 anaesthesia ('down' states) (Toth *et al.*, 2008) and could be a result of reduced inhibitory drive from supragranular and infragranular populations (see above) or of reduced inhibition of VPM cells by the reticular nucleus (Nicolelis & Fanselow, 2002). We have previously shown *in vitro* that a diverse range of disparate anaesthetics also prolong activity in assembly activity evoked from the hippocampus CA1 region (Collins *et al.*, 2007), a property that proved to be specific to anaesthetic agents *per se* and not to other psychoactive substances, including other CNS depressants. Such prolongation of activity may partially serve to slow down or block incoming sensory information, and underlie the lack of sensory awareness experienced during general anaesthesia. This scenario is the opposite effect to that observed during the contrary state of cortical arousal (Nicolelis & Fanselow, 2002; Castro-Alamancos, 2004) in which the overall duration of the evoked response is reduced to optimise the processing of fast, discrete sensory stimuli, such as that commonly received from the whiskers while a rodent is actively palpating an object (Carvell & Simons, 1990).

The shape of the evoked response is constant between levels of anaesthesia

Whilst the temporal parameters discussed above could have been recorded purely using electrophysiological techniques, only optical imaging can provide information on the spatial distribution of activity. Changes in evoked activity within different stages of anaesthesia have previously been examined with VSDI (Berger *et al.*, 2007) but spatial changes were not reported. Anaesthesia was shown to markedly reduce the hyperpolarisation phase of the response (figure 6) which coincides with later components of the SEP response (N2 and P2). There is currently an incomplete understanding of the underlying circuitry that is responsible for this activity (see above) but its abolition could result from weakening of sensory responses earlier in the cortical response sequence. There were also marked changes in the absolute amplitude of the depolarisation phase of the optical responses, yet the shape of the evoked response at this time remained constant between different levels of anaesthesia (figure 8C). In other words, in relation to the central barrel, activity in surrounding barrels remained constant throughout different levels of anaesthesia. Alternatively, by extension, if the external world were indeed represented as a population code, rather than via rate or temporal coding mechanisms, as recent reports suggest (Harris, 2005), the current findings would indicate an identical functional representation of the whisker stimulus in different levels of anaesthesia.

That the intrinsic response pattern is unchanged across anaesthetic levels is reassuring for technical reasons as anaesthetic 'drift' within experimental recording periods, as well as differences in anaesthetic depth between animals, is an often unavoidable occurrence during *in vivo* studies (Angel *et al.*, 1976; Angel, 1991). Consequently, though it is currently somewhat difficult to resolve the differences in response parameters *between*

different anaesthetic agents (Rojas *et al.*, 2006), it appears as though the potential confound that a fluctuating response shape might introduce to data can be ignored (at least with the common anaesthetic agent used in the current study, urethane). This is especially relevant to imaging studies that aim to investigate intracortical signal processing (Petersen *et al.*, 2003; Civillico & Contreras, 2006; Berger *et al.*, 2007) where such fluctuations in baseline response could introduce unnecessary variability into, if not invalidate, the acquired data.

The results presented here are in agreement with previous studies, predominantly using electrophysiology, that have demonstrated state-dependent changes in the temporal profiles (amplitudes) of sensory-evoked responses, but the new finding here relates to the spatial features revealed by optical imaging. Firstly, we observed an interesting effect whereby responses are prolonged under successively deeper levels of anaesthesia. As this latter effect has also been recorded in isolated *in vitro* preparations, and in different brain structures, we speculate that response prolongation may be a more common effect of anaesthesia and, in doing so, may sustain the brain in a state in which it remains unresponsive to incoming sensory information. Secondly, we were able to show that the reduction in amplitude of the assembly, during this period, did not change its relative intrinsic pattern of activity. Though the data presented here provide mere clues as to the action of anaesthetics on the brain, given the importance of network states in a variety of neural functions, especially those that involve states of arousal (Cariani, 2000; Harris, 2005; Krueger *et al.*, 2008) our incomplete understanding of the mechanisms underlying general anaesthesia will no doubt be improved with the application of imaging techniques

such as VSDI and the thorough examination of spatiotemporal components of brain activity.

Acknowledgements

This work was funded by grants from the Mind Science Foundation, John Templeton Foundation and the James Martin 21st Century School. We would like to thank Wendy Tynan and Dr. Sue Totterdell for help with histological processing and two anonymous referees for their helpful and insightful comments.

Abbreviations

Di4-ANEPPS: pyridinium 4-[2-[6-(dibutylamino)-2-naphthalenyl]-ethenyl]-1-(3-sulfopropyl)hydroxide

ECG: electrocardiogram

EEG: electroencephalogram

ROI: region of interest

SEP: somatosensory-evoked potential

VSDI: voltage-sensitive dye imaging

References

Aguilar, J.R. & Castro-Alamancos, M.A. (2005) Spatiotemporal gating of sensory inputs in thalamus during quiescent and activated states. *J Neurosci*, **25**, 10990-11002.

Angel, A. (1991) The G. L. Brown lecture. Adventures in anaesthesia. *Exp Physiol*, **76**, 1-38.

Angel, A., Arnott, R.H., Linkens, D.A. & Ting, C.H. (2000) Somatosensory evoked potentials for closed-loop control of anaesthetic depth using propofol in the urethane-anaesthetized rat. *Br J Anaesth*, **85**, 431-439.

Angel, A., Dodd, J. & Gray, J.D. (1976) Proceedings: Fluctuating anaesthetic state in the rat anaesthetized with urethane. *J Physiol*, **259**, 11P-12P.

Angel, A. & Gratton, D.A. (1982) The effect of anaesthetic agents on cerebral cortical responses in the rat. *Br J Pharmacol*, **76**, 541-549.

Antunes, L.M., Golledge, H.D., Roughan, J.V. & Flecknell, P.A. (2003) Comparison of electroencephalogram activity and auditory evoked responses during isoflurane and halothane anaesthesia in the rat. *Vet Anaesth Analg*, **30**, 15-23.

Armstrong-James, M. & George, M.J. (1988) Influence of anesthesia on spontaneous activity and receptive field size of single units in rat Sm1 neocortex. *Exp Neurol*, **99**, 369-387.

Barth, D.S., Kithas, J. & Di, S. (1993) Anatomic organization of evoked potentials in rat parietotemporal cortex: somatosensory and auditory responses. *J Neurophysiol*, **69**, 1837-1849.

Berger, T., Borgdorff, A., Crochet, S., Neubauer, F.B., Lefort, S., Fauvet, B., Ferezou, I., Carleton, A., Luscher, H.R. & Petersen, C.C. (2007) Combined voltage and calcium epifluorescence imaging in vitro and in vivo reveals subthreshold and suprathreshold dynamics of mouse barrel cortex. *J Neurophysiol*, **97**, 3751-3762.

Bernardo, K.L., McCasland, J.S. & Woolsey, T.A. (1990a) Local axonal trajectories in mouse barrel cortex. *Exp Brain Res*, **82**, 247-253.

Bernardo, K.L., McCasland, J.S., Woolsey, T.A. & Strominger, R.N. (1990b) Local intra- and interlaminar connections in mouse barrel cortex. *J Comp Neurol*, **291**, 231-255.

Buzsaki, G. & Draguhn, A. (2004) Neuronal oscillations in cortical networks. *Science*, **304**, 1926-1929.

Cariani, P. (2000) Anesthesia, neural information processing, and conscious awareness. *Conscious Cogn*, **9**, 387-395.

Carvell, G.E. & Simons, D.J. (1988) Membrane potential changes in rat SmI cortical neurons evoked by controlled stimulation of mystacial vibrissae. *Brain Res*, **448**, 186-191.

Carvell, G.E. & Simons, D.J. (1990) Biometric analyses of vibrissal tactile discrimination in the rat. *J Neurosci*, **10**, 2638-2648.

Castro-Alamancos, M.A. (2004) Dynamics of sensory thalamocortical synaptic networks during information processing states. *Prog Neurobiol*, **74**, 213-247.

Chemla, S. & Chavane, F. (in press) Voltage-sensitive dye imaging: Technique review and models. *J Physiol (Paris)*.

Civillico, E.F. & Contreras, D. (2006) Integration of evoked responses in supragranular cortex studied with optical recordings in vivo. *J Neurophysiol*, **96**, 336-351.

Coenen, A.M. (1995) Neuronal activities underlying the electroencephalogram and evoked potentials of sleeping and waking: implications for information processing. *Neurosci Biobehav Rev*, **19**, 447-463.

Collins, T.F., Mann, E.O., Hill, M.R., Dommett, E.J. & Greenfield, S.A. (2007) Dynamics of neuronal assemblies are modulated by anaesthetics but not analgesics. *Eur J Anaesthesiol*, **24**, 609-614.

Contreras, D. & Llinas, R. (2001) Voltage-sensitive dye imaging of neocortical spatiotemporal dynamics to afferent activation frequency. *J Neurosci*, **21**, 9403-9413.

Derdikman, D., Hildesheim, R., Ahissar, E., Arieli, A. & Grinvald, A. (2003) Imaging spatiotemporal dynamics of surround inhibition in the barrels somatosensory cortex. *J Neurosci*, **23**, 3100-3105.

Devonshire, I.M., Mayhew, J.E. & Overton, P.G. (2007) Cocaine preferentially enhances sensory processing in the upper layers of the primary sensory cortex. *Neuroscience*, **146**, 841-851.

Devonshire, I.M., Preston, M.J., Dommett, E.J., Murphy, K.L. & Greenfield, S.A. (2009) Design and evaluation of a low-cost respiratory monitoring device for use with anaesthetized animals. *Lab Anim*, **43**, 382-389.

Di, S. & Barth, D.S. (1991) Topographic analysis of field potentials in rat vibrissa/barrel cortex. *Brain Res*, **546**, 106-112.

Di, S., Baumgartner, C. & Barth, D.S. (1990) Laminar analysis of extracellular field potentials in rat vibrissa/barrel cortex. *J Neurophysiol*, **63**, 832-840.

Egger, V., Feldmeyer, D. & Sakmann, B. (1999) Coincidence detection and changes of synaptic efficacy in spiny stellate neurons in rat barrel cortex. *Nat Neurosci*, **2**, 1098-1105.

Erchova, I.A., Lebedev, M.A. & Diamond, M.E. (2002) Somatosensory cortical neuronal population activity across states of anaesthesia. *Eur J Neurosci*, **15**, 744-752.

Ferezou, I., Bolea, S. & Petersen, C.C. (2006) Visualizing the cortical representation of whisker touch: voltage-sensitive dye imaging in freely moving mice. *Neuron*, **50**, 617-629.

Franks, N.P. (2008) General anaesthesia: from molecular targets to neuronal pathways of sleep and arousal. *Nat Rev Neurosci*, **9**, 370-386.

Freye, E., Bruckner, J. & Latasch, L. (2004) No difference in electroencephalographic power spectra or sensory-evoked potentials in patients anaesthetized with desflurane or sevoflurane. *Eur J Anaesthesiol*, **21**, 373-378.

Friedberg, M.H., Lee, S.M. & Ebner, F.F. (1999) Modulation of receptive field properties of thalamic somatosensory neurons by the depth of anesthesia. *J Neurophysiol*, **81**, 2243-2252.

Goff, W.R., Allison, T. & Vaughan Jr., H.G. (1978) The functional neuroanatomy of event-related potentials. In Callaway, E., Tueting, P., Koslow, S.H. (eds.) *Event-related brain potentials in man*. Academic Press, New York.

Goss-Sampson, M.A. & Kriss, A. (1991) Effects of pentobarbital and ketamine-xylazine anaesthesia on somatosensory, brainstem auditory and peripheral sensory-motor responses in the rat. *Lab Anim*, **25**, 360-366.

Greenfield, S.A. (2000) *Private Life of the Brain*. John Wiley & Sons, New York.
Grinvald, A., Arieli, A., Tsodyks, M. & Kenet, T. (2003) Neuronal assemblies: single cortical neurons are obedient members of a huge orchestra. *Biopolymers*, **68**, 422-436.
Grinvald, A. & Hildesheim, R. (2004) VSDI: a new era in functional imaging of cortical dynamics. *Nat Rev Neurosci*, **5**, 874-885.
Guedel, A.E. (1920) Signs of inhalational anesthesia. In Guedel, A.E. (ed.) *Inhalational anesthesia*. MacMillan, New York, pp. 10-52.
Haider, B., Duque, A., Hasenstaub, A.R., Yu, Y. & McCormick, D.A. (2007) Enhancement of visual responsiveness by spontaneous local network activity in vivo. *J Neurophysiol*, **97**, 4186-4202.
Harris, K.D. (2005) Neural signatures of cell assembly organization. *Nat Rev Neurosci*, **6**, 399-407.
Hasenstaub, A., Sachdev, R.N. & McCormick, D.A. (2007) State changes rapidly modulate cortical neuronal responsiveness. *J Neurosci*, **27**, 9607-9622.
Hebb, D.O. (1949) *The Organization of Behavior*. Wiley, New York.
Jellema, T., Brunia, C.H. & Wadman, W.J. (2004) Sequential activation of microcircuits underlying somatosensory-evoked potentials in rat neocortex. *Neuroscience*, **129**, 283-295.
Jones, E.G. (1984) Identification and classification of intrinsic circuit elements in the neocortex. In Edelman, G.M., Gall, W.E., Cowan, W.M. (eds.) *Dynamic Aspects of Neocortical Function*. Wiley, New York.
Kisley, M.A. & Gerstein, G.L. (1999) Trial-to-trial variability and state-dependent modulation of auditory-evoked responses in cortex. *J Neurosci*, **19**, 10451-10460.
Kleinfeld, D. & Delaney, K.R. (1996) Distributed representation of vibrissa movement in the upper layers of somatosensory cortex revealed with voltage-sensitive dyes. *J Comp Neurol*, **375**, 89-108.
Koch, C. & Greenfield, S. (2007) How does consciousness happen? *Sci Am*, **297**, 76-83.
Koyanagi, I. & Tator, C.H. (1996) The effects of cortical stimulation, anesthesia and recording site on somatosensory evoked potentials in the rat. *Electroencephalogr Clin Neurophysiol*, **101**, 534-542.
Krueger, J.M., Rector, D.M., Roy, S., Van Dongen, H.P., Belenky, G. & Panksepp, J. (2008) Sleep as a fundamental property of neuronal assemblies. *Nat Rev Neurosci*, **9**, 910-919.
Kuhn, B., Denk, W. & Bruno, R.M. (2008) In vivo two-photon voltage-sensitive dye imaging reveals top-down control of cortical layers 1 and 2 during wakefulness. *Proc Natl Acad Sci U S A*, **105**, 7588-7593.
Kulics, A.T. (1982) Cortical neural evoked correlates of somatosensory stimulus detection in the rhesus monkey. *Electroencephalogr Clin Neurophysiol*, **53**, 78-93.
Kulics, A.T. & Cauller, L.J. (1986) Cerebral cortical somatosensory evoked responses, multiple unit activity and current source-densities: their interrelationships and significance to somatic sensation as revealed by stimulation of the awake monkey's hand. *Exp Brain Res*, **62**, 46-60.
Land, P.W. & Simons, D.J. (1985) Cytochrome oxidase staining in the rat SmI barrel cortex. *J Comp Neurol*, **238**, 225-235.

Lee, S.M., Friedberg, M.H. & Ebner, F.F. (1994) The role of GABA-mediated inhibition in the rat ventral posterior medial thalamus. II. Differential effects of GABAA and GABAB receptor antagonists on responses of VPM neurons. *J Neurophysiol*, **71**, 1716-1726.

Lin, L., Osan, R. & Tsien, J.Z. (2006) Organizing principles of real-time memory encoding: neural clique assemblies and universal neural codes. *Trends Neurosci*, **29**, 48-57.

Lippert, M.T., Takagaki, K., Xu, W., Huang, X. & Wu, J.Y. (2007) Methods for voltage-sensitive dye imaging of rat cortical activity with high signal-to-noise ratio. *J Neurophysiol*, **98**, 502-512.

Ma, H.T., Wu, C.H. & Wu, J.Y. (2004) Initiation of spontaneous epileptiform events in the rat neocortex in vivo. *J Neurophysiol*, **91**, 934-945.

Mayhew, J., Johnston, D., Berwick, J., Jones, M., Coffey, P. & Zheng, Y. (2000) Spectroscopic analysis of neural activity in brain: increased oxygen consumption following activation of barrel cortex. *Neuroimage*, **12**, 664-675.

Mitzdorf, U. (1985) Current source-density method and application in cat cerebral cortex: investigation of evoked potentials and EEG phenomena. *Physiol Rev*, **65**, 37-100.

Ngai, A.C., Jolley, M.A., D'Ambrosio, R., Meno, J.R. & Winn, H.R. (1999) Frequency-dependent changes in cerebral blood flow and evoked potentials during somatosensory stimulation in the rat. *Brain Res*, **837**, 221-228.

Nicholson, C. & Freeman, J.A. (1975) Theory of current source-density analysis and determination of conductivity tensor for anuran cerebellum. *J Neurophysiol*, **38**, 356-368.

Nicolelis, M.A. & Fanselow, E.E. (2002) Thalamocortical [correction of Thalamcortical] optimization of tactile processing according to behavioral state. *Nat Neurosci*, **5**, 517-523.

Nicolelis, M.A., Fanselow, E.E. & Ghazanfar, A.A. (1997) Hebb's dream: the resurgence of cell assemblies. *Neuron*, **19**, 219-221.

Oldford, E. & Castro-Alamancos, M.A. (2003) Input-specific effects of acetylcholine on sensory and intracortical evoked responses in the "barrel cortex" in vivo. *Neuroscience*, **117**, 769-778.

Petersen, C.C., Grinvald, A. & Sakmann, B. (2003) Spatiotemporal dynamics of sensory responses in layer 2/3 of rat barrel cortex measured in vivo by voltage-sensitive dye imaging combined with whole-cell voltage recordings and neuron reconstructions. *J Neurosci*, **23**, 1298-1309.

Reyes, A. & Sakmann, B. (1999) Developmental switch in the short-term modification of unitary EPSPs evoked in layer 2/3 and layer 5 pyramidal neurons of rat neocortex. *J Neurosci*, **19**, 3827-3835.

Rojas, M.J., Navas, J.A. & Rector, D.M. (2006) Evoked response potential markers for anesthetic and behavioral states. *Am J Physiol Regul Integr Comp Physiol*, **291**, R189-196.

Sachdev, R.N., Ebner, F.F. & Wilson, C.J. (2004) Effect of subthreshold up and down states on the whisker-evoked response in somatosensory cortex. *J Neurophysiol*, **92**, 3511-3521.

Schmidt, G.N., Scharein, E., Siegel, M., Muller, J., Debener, S., Nitzschke, R., Engel, A. & Bischoff, P. (2007) Identification of sensory blockade by somatosensory and pain-induced evoked potentials. *Anesthesiology*, **106**, 707-714.

Shirvalkar, P.R. (2009) Hippocampal neural assemblies and conscious remembering. *J Neurophysiol*, **101**, 2197-2200.

Shoham, D., Glaser, D.E., Arieli, A., Kenet, T., Wijnbergen, C., Toledo, Y., Hildesheim, R. & Grinvald, A. (1999) Imaging cortical dynamics at high spatial and temporal resolution with novel blue voltage-sensitive dyes. *Neuron*, **24**, 791-802.

Steriade, M. (1984) The excitatory-inhibitory response sequence in thalamic and neocortical cells: state-related changes and regulatory systems. In Edelman, G.M., Gall, W.E., Cowan, W.M. (eds.) *Dynamic Aspects of Neocortical Function*. Wiley, New York.

Sukov, W. & Barth, D.S. (1998) Three-dimensional analysis of spontaneous and thalamically evoked gamma oscillations in auditory cortex. *J Neurophysiol*, **79**, 2875-2884.

Takashima, I., Kajiwara, R. & Iijima, T. (2001) Voltage-sensitive dye versus intrinsic signal optical imaging: comparison of optically determined functional maps from rat barrel cortex. *Neuroreport*, **12**, 2889-2894.

Toth, A., Gyengesi, E., Zaborszky, L. & Detari, L. (2008) Interaction of slow cortical rhythm with somatosensory information processing in urethane-anesthetized rats. *Brain Res*, **1226**, 99-110.

Wu, J.Y., Xiaoying, H. & Chuan, Z. (2008) Propagating waves of activity in the neocortex: what they are, what they do. *Neuroscientist*, **14**, 487-502.

Zheng, Y., Johnston, D., Berwick, J. & Mayhew, J. (2001) Signal source separation in the analysis of neural activity in brain. *Neuroimage*, **13**, 447-458.

Figure legends

Figure 1. Levels of anaesthesia. Supplemental doses of anaesthetic were administered to gradually increase the depth of anaesthesia from a 'light' stage (A) to 'moderate' (B) to 'deep' (C); representative data from a single animal is shown. Different levels of anaesthesia could be distinguished by eye: light anaesthesia exhibited a marked decrease in amplitude versus moderate; deep anaesthesia exhibited periods of burst-suppression. Nevertheless, the mean power frequency of the pre-stimulus EEG was used to automatically divide response trials into different anaesthetic levels using fast Fourier transforms (FFT; D). FFT data is the average of all trials across all animals (n=7).

Figure 2. Illustration of origins of SEP and VSDI time courses from a single animal. A: Image of barrel cortex under 590nm illumination; electrode used for SEP (and EEG) recordings can be clearly seen). B: Snapshot of activation 8 ms after whisker deflection; inset displays the 'shape' of the response, obtained by locating the pixel with maximum activation, bisecting the image horizontally and vertically across this pixel and averaging the resultant vectors. C: Area of supra-threshold activation (20% of the maximum response) 8 ms after stimulation. D: Typical SEP response with each individual component (P1, N1, P2, N2) indicated; also shows how amplitude of each was calculated (dashed lines). E: VSDI time course obtained using the region-of-interest shown in B with a grey circle (centred over the maximally activated pixel). Positive and negative peaks are indicated, that are used in further analysis. F: Extent of spatial activation over time (in pixels), base on supra-threshold pixel activation exemplified in C.

Figure 3. Time course plots of SEP and VSDI responses during light anaesthesia. Responses to 2 Hz (A & C) and 10 Hz (B & D) stimulus frequencies are shown, SEP in the upper plots (A & B); VSDI in the lower plots (C & D). The three response types used in further analyses are marked at the bottom of the figure: stand-alone, low-frequency and high-frequency.

Figure 4. Time course plots of SEP and VSDI responses during different states of anaesthesia. Response types are shown vertically; A&D: stand-alone stimulus; B&E: low-frequency; C&F: high-frequency; SEP responses are shown in the upper panels (A-C), VSDI responses in the lower panels (D-F). Inset of D illustrates the timing of initial SEP and VSDI response components.

Figure 5. Amplitudes of SEP and VSDI responses in different levels of anaesthesia. Response types are shown vertically; A&D: stand-alone stimulus; B&E: low-frequency; C&F: high-frequency; SEP responses are shown in the upper panels (A-C), VSDI responses in the lower panels (D-F). Responses have been normalized to the response evoked under light anaesthesia for each response component on which one-way ANOVAs were performed. Error bars represent standard error of the mean (n=7); asterisks represent results of least significant difference post-hoc tests (* = $p < 0.05$; ** = $p < 0.01$).

Figure 6. VSDI activation patterns evoked by stand-alone whisker stimulation during light (A) and deep (B) levels of anaesthesia. Time after stimulus onset is displayed in upper right corners; note change in time intervals in second and third rows. Time course in the lower right corner of each panel illustrates the response from the centre of the image; tick marks beneath the plot illustrate the portions of the response that are shown in the images (interval between the first two ticks shown in images on the first row; interval between last two ticks in the expanded time images shown on the second and third rows). Colormap represents normalised change in the optical signal (data were normalised to the maximally activated pixel); data shown are averages from all animals with each image centralised on the pixel exhibiting the maximum response (n=7). Scale bar = 500 μm.

Figure 7. Spatiotemporal dynamics of the spreading response in different levels of anaesthesia in response to stand-alone stimulation. A: cortical area activated by stimulation, calculated by including pixels that were greater than 20% of the maximum response (or minimum in the case of the negative, or hyperpolarisation, phase of the response) that was elicited in each animal across all three levels of anaesthesia. B:

maximum area activated during depolarisation and hyperpolarisation phases of the response. Responses in B have been normalized to the response evoked under light anaesthesia for each response component. Positive response, $F = 4.433$, $p < 0.05$; negative response, $F = 9.501$, $p < 0.05$. Error bars represent standard error of the mean (n=7); asterisks represent results of least significance difference post-hoc tests (* = $p < 0.05$; ** = $p < 0.01$).

Figure 8. Three-dimensional shape of response and location with respect to anatomically-defined barrels. A: activation profile at 4 ms post-stimulus onset from a single animal to show the concordance with the C2 barrel (during light anaesthesia); colormap represents percentage change in the optical signal. B: tangential section of barrel cortex layer IV stained for cytochrome oxidase reactivity; C-F: VSDI response shape at four time points for at each anaesthetic level. Plots produced by locating the pixel with maximum activation in each animal, bisecting the image in two dimensions across this pixel (vertical and horizontal) and averaging the resultant vectors to provide an outline of the shape of the assembly, from centre to periphery (L to R). Error bars represent standard error of the mean (n=7). Scale bar = 500 μm.

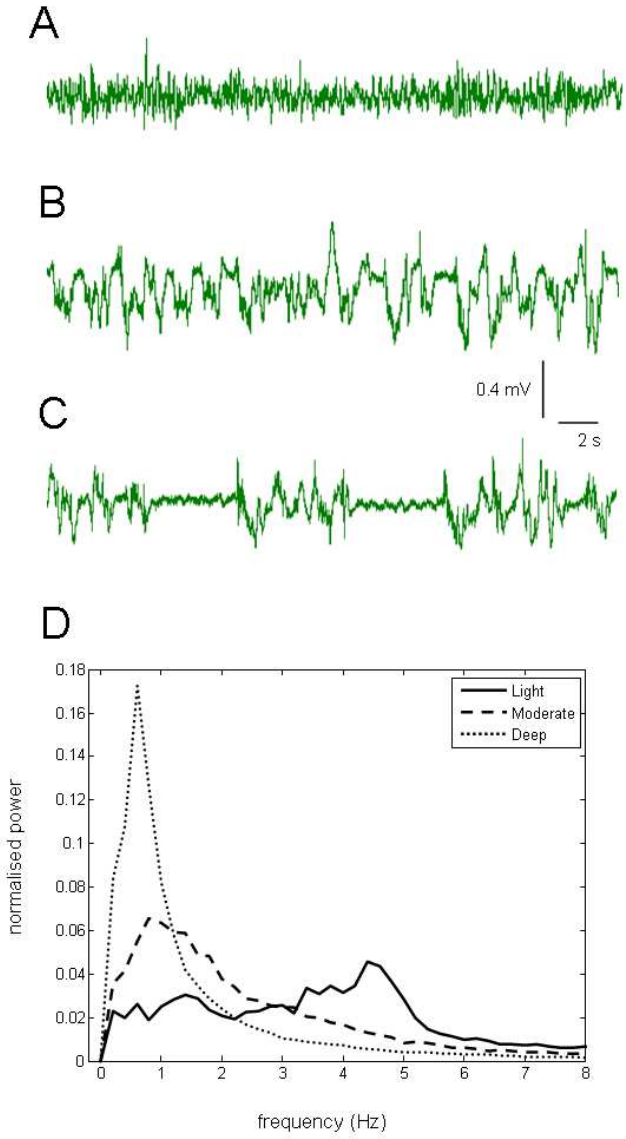

Figure 1. Levels of anaesthesia. Supplemental doses of anaesthetic were administered to gradually increase the depth of anaesthesia from a 'light' stage (A) to 'moderate' (B) to 'deep' (C); representative data from a single animal is shown. Different levels of anaesthesia could be distinguished by eye: light anaesthesia exhibited a marked decrease in amplitude versus moderate; deep anaesthesia exhibited periods of burst-suppression. Nevertheless, the mean power frequency of the pre-stimulus EEG was used to automatically divide response trials into different anaesthetic levels using fast Fourier transforms (FFT; D). FFT data is the average of all trials across all animals (n=7).
100x172mm (150 x 150 DPI)

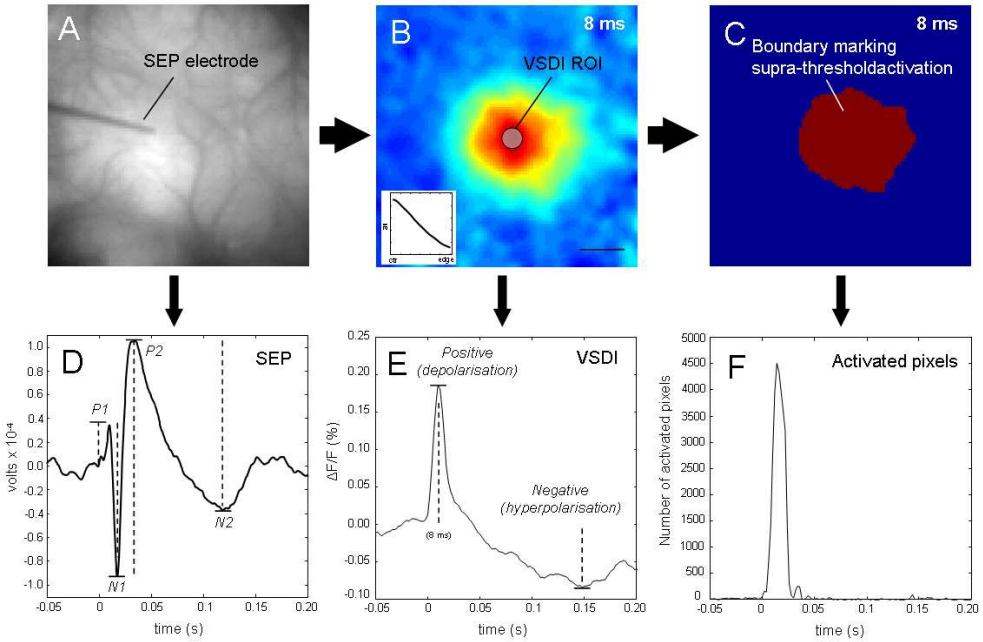

Figure 2. Illustration of origins of SEP and VSDI time courses from a single animal. A: Image of barrel cortex under 590nm illumination; electrode used for SEP (and EEG) recordings can be clearly seen). B: Snapshot of activation 8 ms after whisker deflection; inset displays the 'shape' of the response, obtained by locating the pixel with maximum activation, bisecting the image horizontally and vertically across this pixel and averaging the resultant vectors. C: Area of supra-threshold activation (20% of the maximum response) 8 ms after stimulation. D: Typical SEP response with each individual component (P1, N1, P2, N2) indicated; also shows how amplitude of each was calculated (dashed lines). E: VSDI time course obtained using the region-of-interest shown in B with a grey circle (centred over the maximally activated pixel). Positive and negative peaks are indicated, that are used in further analysis. F: Extent of spatial activation over time (in pixels), base on supra-threshold pixel activation exemplified in C.
194x130mm (150 x 150 DPI)

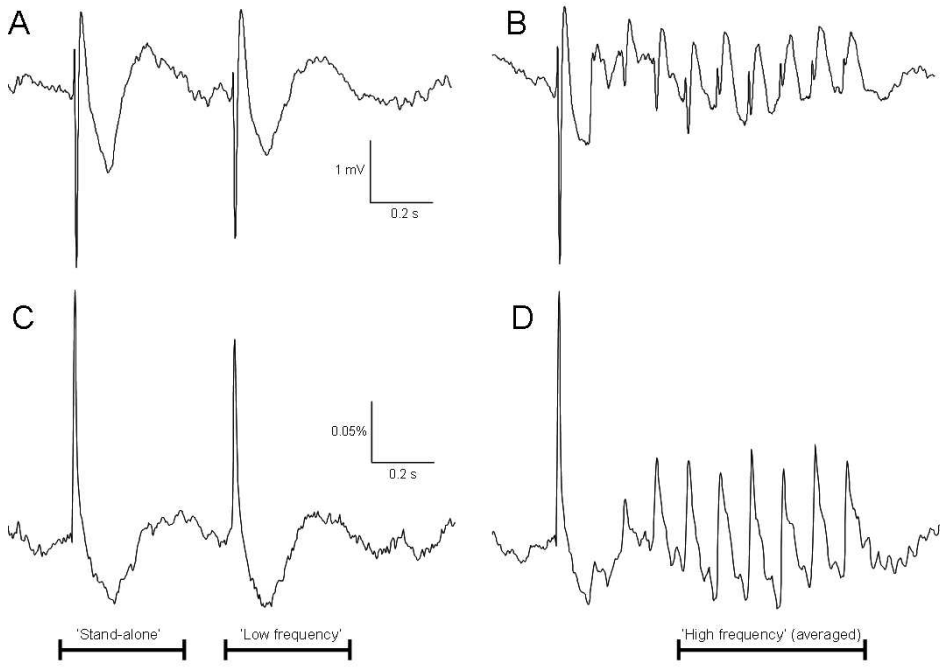

Figure 3. Time course plots of SEP and VSDI responses during light anaesthesia. Responses to 2 Hz (A & C) and 10 Hz (B & D) stimulus frequencies are shown, SEP in the upper plots (A & B); VSDI in the lower plots (C & D). The three response types used in further analyses are marked at the bottom of the figure: stand-alone, low-frequency and high-frequency.
193x130mm (150 x 150 DPI)

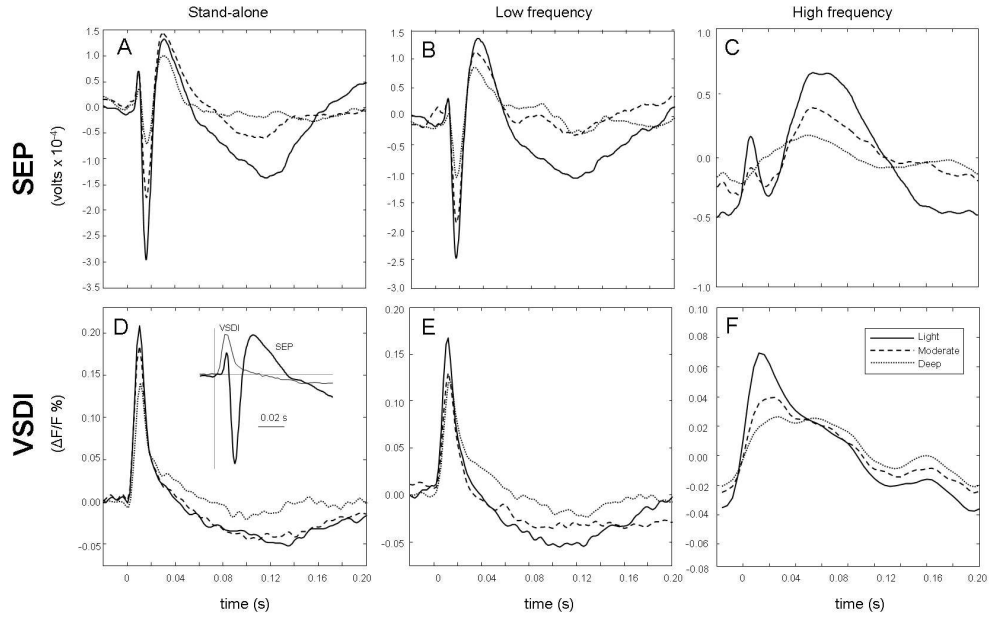

Figure 4. Time course plots of SEP and VSDI responses during different states of anaesthesia. Response types are shown vertically; A&D: stand-alone stimulus; B&E: low-frequency; C&F: high-frequency; SEP responses are shown in the upper panels (A-C), VSDI responses in the lower panels (D-F). Inset of D illustrates the timing of initial SEP and VSDI response components.
285x181mm (150 x 150 DPI)

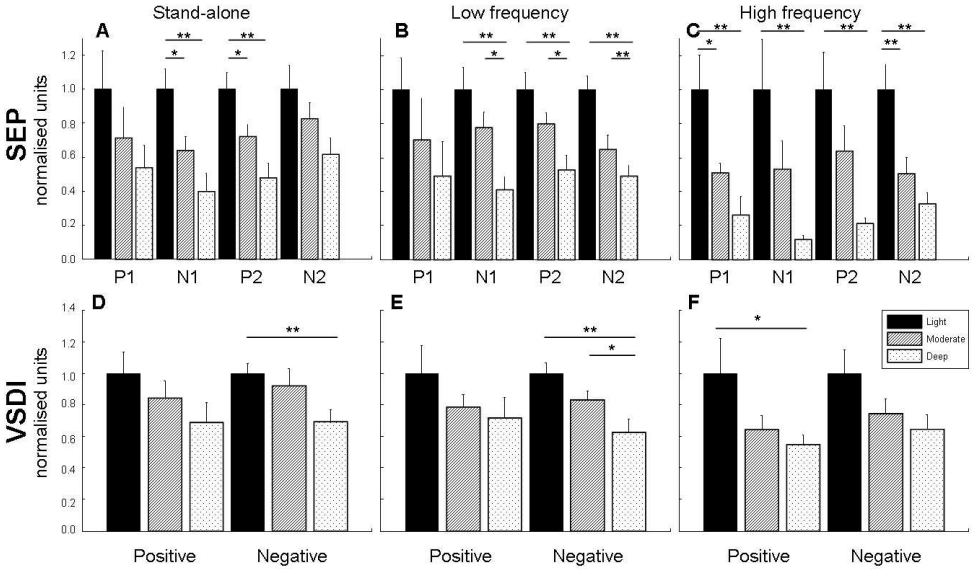

Figure 5. Amplitudes of SEP and VSDI responses in different levels of anaesthesia. Response types are shown vertically; A&D: stand-alone stimulus; B&E: low-frequency; C&F: high-frequency; SEP responses are shown in the upper panels (A-C), VSDI responses in the lower panels (D-F). Responses have been normalized to the response evoked under light anaesthesia for each response component on which one-way ANOVAs were performed. Error bars represent standard error of the mean (n=7); asterisks represent results of least significant difference post-hoc tests (* = $p < 0.05$; ** = $p < 0.01$).
234x138mm (150 x 150 DPI)

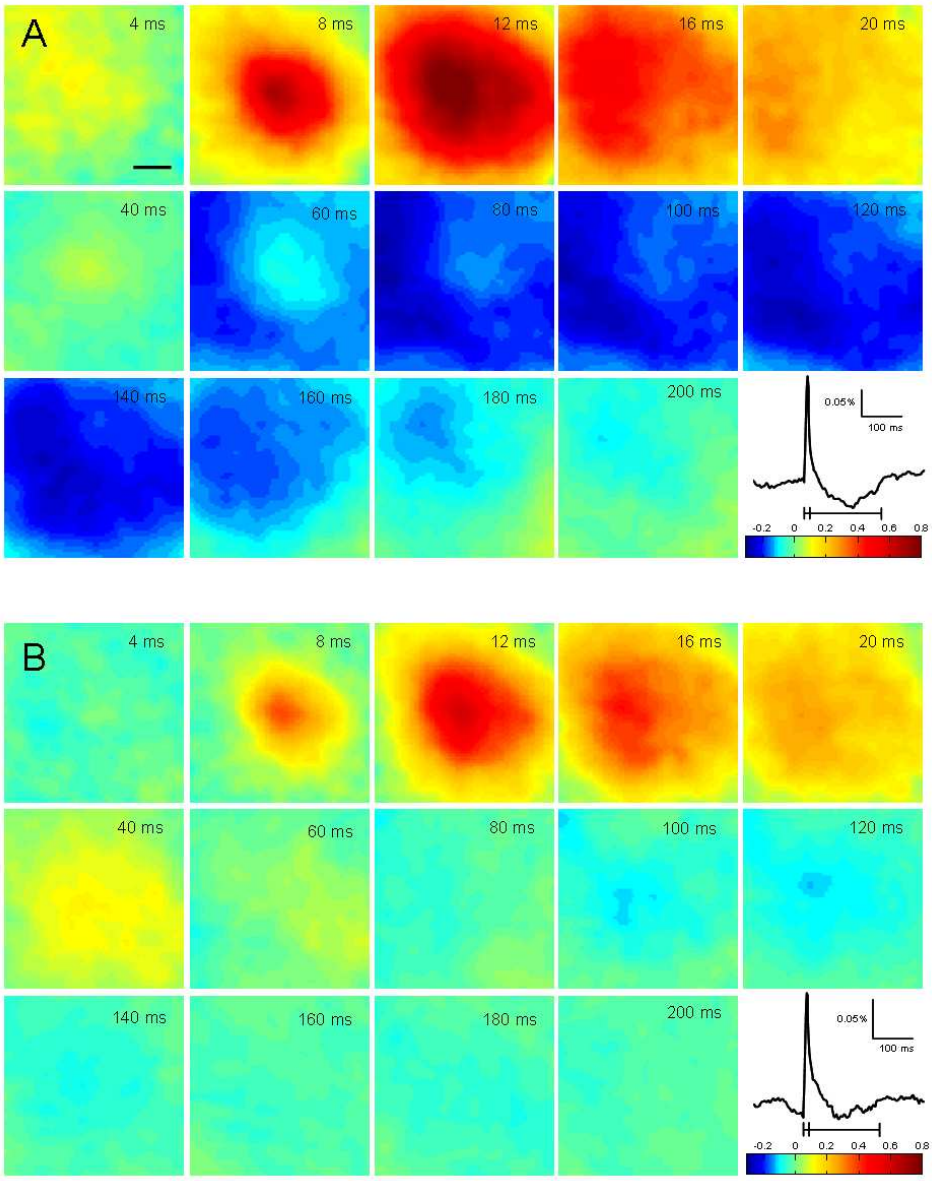

Figure 6. VSDI activation patterns evoked by stand-alone whisker stimulation during light (A) and deep (B) levels of anaesthesia. Time after stimulus onset is displayed in upper right corners; note change in time intervals in second and third rows. Time course in the lower right corner of each panel illustrates the response from the centre of the image; tick marks beneath the plot illustrate the portions of the response that are shown in the images (interval between the first two ticks shown in images on the first row; interval between last two ticks in the expanded time images shown on the second and third rows). Colormap represents normalised change in the optical signal (data were normalised to the maximally activated pixel); data shown are averages from all animals with each image centralised on the pixel exhibiting the maximum response (n=7). Scale bar = 500 μm.
159x200mm (150 x 150 DPI)

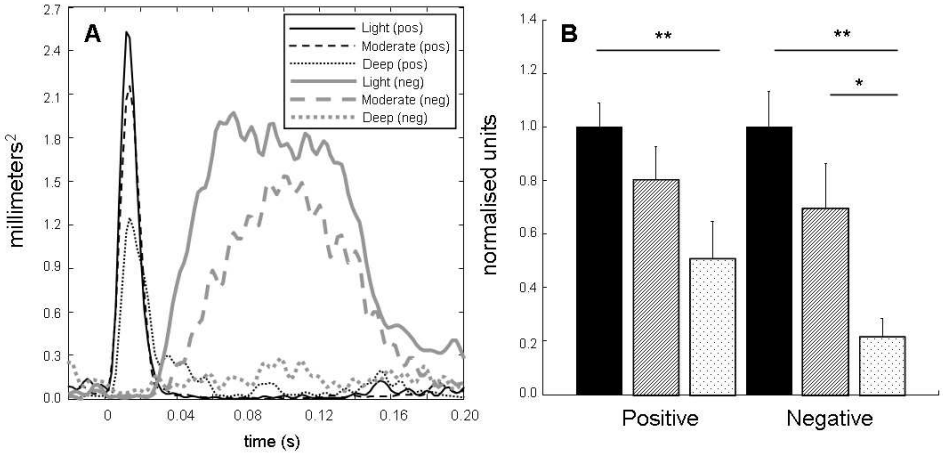

Figure 7. Spatiotemporal dynamics of the spreading response in different levels of anaesthesia in response to stand-alone stimulation. A: cortical area activated by stimulation, calculated by including pixels that were greater than 20% of the maximum response (or minimum in the case of the negative, or hyperpolarisation, phase of the response) that was elicited in each animal across all three levels of anaesthesia. B: maximum area activated during depolarisation and hyperpolarisation phases of the response. Responses in B have been normalized to the response evoked under light anaesthesia for each response component. Positive response, $F = 4.433$, $p < 0.05$; negative response, $F = 9.501$, $p < 0.05$. Error bars represent standard error of the mean (n=7); asterisks represent results of least significance difference post-hoc tests (* = $p < 0.05$; ** = $p < 0.01$).
190x95mm (150 x 150 DPI)

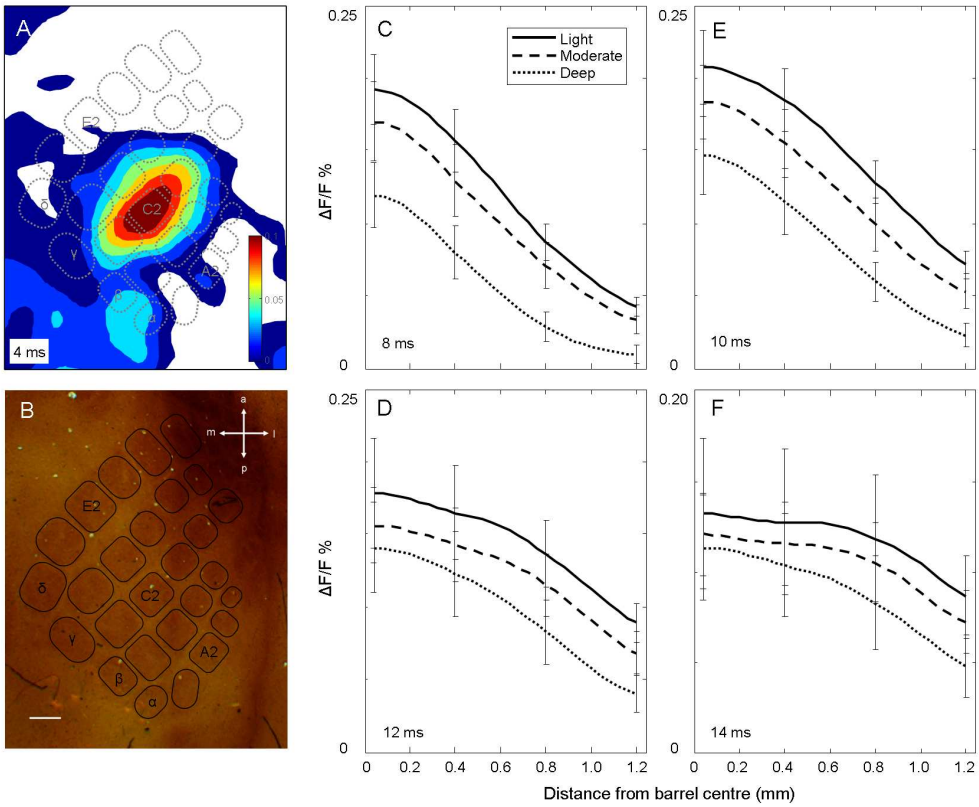

Figure 8. Three-dimensional shape of response and location with respect to anatomically-defined barrels. A: activation profile at 4 ms post-stimulus onset from a single animal to show the concordance with the C2 barrel (during light anaesthesia); colormap represents percentage change in the optical signal. B: tangential section of barrel cortex layer IV stained for cytochrome oxidase reactivity; C-F: VSDI response shape at four time points for at each anaesthetic level. Plots produced by locating the pixel with maximum activation in each animal, bisecting the image in two dimensions across this pixel (vertical and horizontal) and averaging the resultant vectors to provide an outline of the shape of the assembly, from centre to periphery (L to R). Error bars represent standard error of the mean (n=7). Scale bar = 500 μm.
287x238mm (150 x 150 DPI)